PAPER

Bottom-up design of high-energy-density molecules (N2CO)n (n = 2–8)†

Jing-fan Xin,[ab] Fei-fei He[a] and Yi-hong Ding*[a]

Seeking high-energy-density materials (HEDMs) with balanced huge energy release and good stability has remained quite a tough task for both experimentalists and theoreticians. The current HEDM design mostly concentrates on the chemical modification of either the skeletons or ligands. To increase the number of HEDM candidates, a novel design strategy is highly desired. In this paper, we computationally proposed a bottom-up strategy, *i.e.*, a suitable HEDM seed (*e.g.*, cyc-N_2CO) can form novel HEDMs while retaining good stability and good performance. Starting from the experimentally known diazirinone (cyc-N_2CO) as a "seed" and by considering various bond-addition channels (2 + 2/2 + 3/3 + 3 cyclo-addition at the $N=N/C=O/C-N$ bonds), we found that the cyc-N_2CO dimer isomer **1** (*i.e.*, $(N_2CO)_2$ containing a COCO ring with an exocyclic side-N_2 at each C-atom) possess the rate-determining barrier of 29.9 kcal mol^{-1} and exothermicity of 168.7 kcal mol^{-1} into $2N_2 + 2CO$ at the composite CBS-QB3 level. Moreover, the trimer and tetramer of cyc-N_2CO each possess high rate-determining barriers of 25.8 and 30.3 kcal mol^{-1}, respectively, at the CBS-QB3 level. Even higher oligomers with $n = 5–8$ have rate-determining barriers around 25 and 34 kcal mol^{-1}. The spiral skeletons were shown to have a contribution to their good inherent kinetic stability. By comparing the detonation properties with some known HEDM compounds, the oligomers of cyc-N_2CO may well deserve future synthetic trials for novel HEDMs. Our designed $(N_2CO)_n$ with all the untouched $N=N$ bonds differed sharply from the recently reported high-pressure polymerized forms, in which all the double bonds have been transformed into single bonds. The present bottom-up strategy from an HEDM seed (*i.e.*, cyc-N_2CO) to novel oligomeric HEDMs confirmed by the CBS-QB3 calculations seems to be quite promising and may open a new way of designing in the HEDM realm.

1. Introduction

There has been considerable interest in the high-energy-density materials (HEDMs) for decades due to their potential applications in various fields, *e.g.*, propellants, pyrotechnics, and explosives.[1–8] Yet in spite of the great synthetic difficulties (*e.g.*, suitable precursor, suitable stabilization technique, *etc.*), one clear obstacle in the development of energetic materials is the very limited number of HEDM targets. A well-known issue in the HEDM realm is that the designed compounds should in general satisfy two requirements, *i.e.*, high exothermicity and a high barrier. The first requirement necessitates a large heat release upon decomposition, while the second needs a considerable rate-determining decomposition barrier to ensure good kinetic stability. Unfortunately, the two requirements seem to be quite contradictive since in many cases, a thermodynamically

unstable structure would usually be kinetically unstable. Therefore, successful design of a promising HEDM is a great challenge to chemists' mental imagination.

To accelerate rational design of novel molecules that could satisfy both critical HEDM requirements, clever chemists have thought out an "economic and efficient" strategy to generate new and more complex HEDMs by substituting the framework or ligands of known HEDMs[9–12] In such a strategy, the inherent large exothermicity and good kinetic stability of the parent HEDM molecule can be inherited to the new HEDMs by suitable isovalent or analogous skeleton/ligand modifications. Nice examples include the tetrazole derivatives with fused energetic groups (catenated nitrogen atoms) and insensitive fragments,[13] new HEDMs based on N-heterocyclic frameworks,[14] high-energy metal–organic frameworks (HE-MOFs) based on various nitrogen-rich energetic ligands.[15] Note that most HEDM designs concentrate on the nitrogen-content and high heat, whereas the kinetic factor that is associated with the stability has been much less studied especially for systems with larger size.

Is there any alternative designing strategy viable for novel HEDM? We propose that for some monomeric HEDMs with multiple bonds, the bond-addition might be feasible to expand

[a]*Laboratory of Theoretical and Computational Chemistry, Institute of Theoretical Chemistry, Jilin University, Changchun 130023, P. R. China. E-mail: yhdd@jlu.edu.cn*
[b]*Inner Mongolia Key Laboratory of Photoelectric Functional Materials, College of Chemistry and Chemical Engineering, Chifeng University, Chifeng 024000, P. R. China*

the monomer into more energetic and larger-size HEDMs if good kinetic stability can be preserved. Such a strategy mimics the so-called "bottom-up" strategy, which has been hotly pursued in the cluster-assembled material science.[16–18] To testify our proposal, we considered a tetra-atomic molecule N_2CO, which has received considerable computational and experimental attention.[19–31] Of its isomer, a three-membered ring diazirinone (cyc-N_2CO) was first predicted in 1994 as a promising HEDM,[19] with its definitive experimental confirmation in 2011 via the decomposition of gaseous $OC(N_3)_2$ followed by IR spectrum characterization.[26] In this work, we for the first time designed a series of oligomeric HEDMs $(N_2CO)_n$ only with the $C{=}O$ bonds transformed into single bonds, which show marked contrast to the high-pressure polymerized $(N_2CO)_n$ with all multiple bonds transformed into single bonds. The good kinetic stability (around 30 kcal mol^{-1}) of the designed $(N_2CO)_n$ oligomers was confirmed by the composite CBS-QB3 calculations.

2. Computational methods

All calculations were carried out using Gaussian03 and Gaussian09 program packages.[32] The geometric optimization and frequency calculations of both the isomers and transition states were initially carried out at the B3LYP/6-31G(d) level. For structural and energy refinement, the composite CBS-QB3 method[33,34] was applied, which used the B3LYP/6-311G(2d,d,p) geometries and frequencies and computes a series of high-level single-point energy calculations. The eventual energy has been designed to reach the complete basis set (CBS) limit. The connection of each transition state to associated isomers or fragments was checked by the intrinsic reaction coordinate (IRC) method at the B3LYP/6-31G(d) level. In some cases where the structure might experience significant multi-reference character, the broken symmetry strategy,[35] $i.e.$, UB3LYP/6-311G(2d,d,p) with the "guess = (mix, always) keyword, was performed for geometrical optimization (note that for such open-shell singlet calculations, the composite CBS-QB3 calculations are not available at present). To get detailed orbital information, we performed the natural bond orbital (NBO) analysis. The atom coordinate and the critical transition state coordinate of $(N_2CO)_n$ (n = 2–8) are listed in ESI (see Tables S1–S7†).

3. Results and discussions

The discussions are organized as follows. First, we explored the structures and relative energies of various $(cyc$-$N_2CO)_2$ isomers in detail, followed by the isomerization or decomposition pathways of each isomer. Second, based on the most feasible type of kinetically stabilized $(cyc$-$N_2CO)_2$, we discussed the heat release and kinetic stability of higher oligomeric cyc-N_2CO, $i.e.$, $(cyc$-$N_2CO)_n$ (n = 3–8). Third, we predicted the detonation properties and impact sensitivity for $(cyc$-$N_2CO)_n$ (n = 2–8). Finally, implications of the present work were discussed.

3.1 cyc-N_2CO dimer

3.1.1 Isomers. The symmetric cyc-N_2CO has three types of bonds, $i.e.$, $N{=}N$, $C{=}O$ and C–N. In principle, nine bond-addition structures can be initially designed for dimerization of cyc-N_2CO at the B3LYP/6-31G(d) level (see Table 1). The $N{=}N/N{=}N$ addition does not lead to an N–N singly-bonded N_4-ring isomer. Instead, the optimization collapses to the C–N/N–C addition isomer with a puckered six-membered-ring isomer **7** with two $N{=}N$ bonds at the B3LYP/6-31G(d) level. The C–N/N–C ($trans$) and C–N/C–N (cis) addition lead to the six-membered ring isomers **7** and **8**, respectively at the B3LYP/6-31G(d) level. Yet, both isomers disappear at the B3LYP/6-311G(2d,d,p) level, resulting in the fragmentation into $2N_2$ + 2CO. The two four-membered-ring isomers **1** and **2** are formed by the $trans$- and cis-addition of two $C{=}O$ bonds within N_2CO. Due to the strong lone pair repulsions between two neighboring O-atoms, the cis-isomer **2** is thermodynamically less stable than the $trans$-isomer **1** by more than 50 kcal mol^{-1} (higher relative energy means lower thermodynamic stability). The $C{=}O/N{=}N$ addition gives the five-membered-ring isomer **4**, in which the additioned $N{=}N$ bond is completely broken to be non-bonding. The $C{=}O/C$–N and $C{=}O/N$–C addition would lead to the isomers **3** and **5**, respectively.

3.1.2 Kinetic stability. An ideal molecular HEDM must be thermodynamically unstable (high energy) and kinetically stable (high barrier). As listed in Table 1, the optimized five cyc-N_2CO dimers (**1–5**) lie around or within ±60 kcal mol^{-1} with respect to $2cyc$-N_2CO. Since the monomer cyc-N_2CO already has the fragmentation exothermicity of 89.4 kcal mol^{-1} at the CBS-QB3 level, it's no problem that all of them have high energy with respect to $2N_2$ + 2CO. Then, the problem remains in the intrinsic barrier. To determine this key issue, we considered various decomposition pathways as shown in Table 2. Isomers **6–8** that can only exist at the B3LYP/6-31G(d) level are kinetically of no interest since their N_2-extrusion barriers are only 0.2, 0.02 and 0.56 kcal mol^{-1}, respectively at the same level. For simplicity, we only discuss the lowest-energy fragmentation channel of **1–5**.

As shown in Table 2, the isomers **4** and **5** formed by the respective $C{=}O/N{=}N$ and $C{=}O/N$–C addition have negligible kinetic stability, $i.e.$, −1.7 and 0.96 kcal mol^{-1} at the CBS-QB3 level. They should be of no interest even for spectroscopic detection. The slightly negative value for isomer **4** is clearly a result of the composite CBS-QB3 calculation, in which the higher-level energy is computed based on the geometry of a different level. For the isomers **2** and **3** that are formed via the respective $C{=}O/C{=}O$ and $C{=}O/C$–N addition, their most feasible decomposition transition states have certain open-shell singlet characteristics. They have the barriers of 13.9 and 17.4 kcal mol^{-1}, respectively at the UB3LYP/6-311G(2d,d,p) level. For isomer **2**, the RHF → UHF energy lowering value of 7.2 kcal mol^{-1} is considerable, whereas that (0.5 kcal mol^{-1}) for isomer **3** is negligible. The corresponding CBS-QB3 barriers at the restricted level are 19.8 and 22.2 kcal mol^{-1} for **2** and **3**. We expect the rate-determining barriers of **2** and **3** to be around 15 kcal mol^{-1} at the correlated level, which could allow them to be

Table 1 The bond-addition modes of cyc-N_2CO dimers. The relative energies (kcal mol^{-1}) are at the B3LYP/6-311G(2d,d,p) and CBS-QB3 levels (in parenthesis)
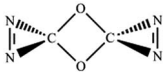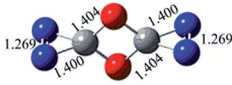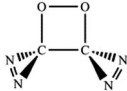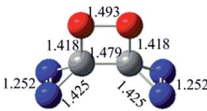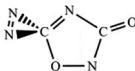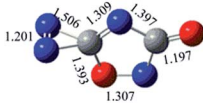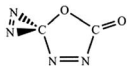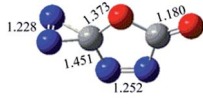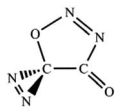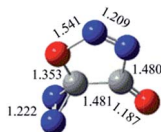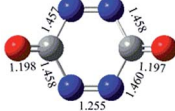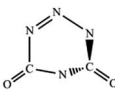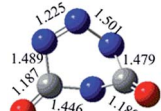
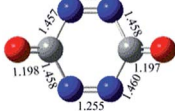| Bond-addition modes	Designed structures of (cyc-N_2CO)$_2$	Optimized structures of (cyc-N_2CO)$_2$	Relative energies between isomers and 2cyc-N_2CO
C=O,O=C (*trans-*)		isomer **1**	−10.0 (−3.4)
C=O,C=O (*cis-*)		isomer **2**	45.9 (52.7)
C=O,N=N		isomer **4**	−7.3 (−5.0)
C=O,C−N (*trans-*)		isomer **3**	−61.2 (−59.5)
C=O,N−C (*cis-*)		isomer **5**	−34.8 (−33.4)
N=N,N=N		isomer **7×**[a]	−46.9[a]
N=N,C−N		isomer **6×**[a]	−51.2[a]
C−N,N−C (*trans-*)		isomer **7×**[a]	−46.9[a]

Table 1 (Contd.)

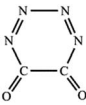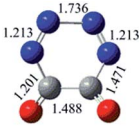| Bond-addition modes	Designed structures of (cyc-N₂CO)₂	Optimized structures of (cyc-N₂CO)₂	Relative energies between isomers and 2cyc-N₂CO
C–N,C–N (cis-)		isomer **8×**[a]	−35.9[a]

[a] The structure is only a minimum at the B3LYP/6-31G(d) level.

detectable in future spectroscopic studies. In sharp contrast, the highly symmetric isomer **1** (D_{2d}) have very high decomposition barriers, *i.e.*, 29.9 (**1-TS1**) and 42.9 (**1-TS2**) kcal mol^{-1} at the CBS-QB3 level for the fragmentation to N₂-leaving and 2cyc-N₂CO, respectively (see Table 2). Clearly, isomer **1** is the most kinetically stable among all the *cyc*-N₂CO dimers.

It should be noted that for the associated fragments, *i.e.*, linear CNN and O₂, their triplet states are energetically more stable than the corresponding singlet ones by 28.91 and 39.02 kcal mol^{-1}, respectively. So, possible singlet → triplet intersystem crossing (ISC) of the associated fragmentation channels needs to be considered. As examples, at the B3LYP/6-311G(2d,d,p) level, the triplet (*cyc*-N₂CO)₂ isomers ^{3}**1**–^{3}**4** and their decomposition transition states were optimized. The rate-determining barriers of ^{3}**1**–^{3}**4** are only 4.2, 6.8, 3.0 and 0.2 kcal mol^{-1}, respectively. This indicates the shallowness of the triplet energy surface of (*cyc*-N₂CO)₂. Yet, more importantly, all the triplet (*cyc*-N₂CO)₂ isomers lie significantly higher than the singlet isomers and the related rate-determining transition states in square brackets, *i.e.*, 56.9 [25.5], 53.9 [30.8], 52.9 [35.0] and 29.7 [26.9] kcal mol^{-1} for **1**, **2**, **3** and **4**, respectively. So there would be no intersystem crossing prior to the singlet fragmentation transition state, and would not affect the kinetic stability of the singlet (*cyc*-N₂CO)₂ isomers. For details, see Table S8 in ESI.† We expect that the same conclusion should hold for higher oligomers of *cyc*-N₂CO.

3.1.3 Structural and electronic feature of isomer 1. The very good kinetic stability of the tricyclic isomer **1** can find support from its unique geometrical and electronic features. The central COCO-ring is spirally connected to the two neighboring CNN-rings, *i.e.*, the center ring is perpendicular to the connected rings. With the N=N bond retained, there exists a set of π-bonding orbital within each CNN-ring. Meanwhile, there are four π-type lone-pairs at two O-atoms within the COCO-ring (see HOMO-8 in Fig. 1). Consequently, both the π-type lone-pair (COCO-ring) and N=N double bonding (CNN-ring) orbitals can conjugate with the exocyclic C–N (CNN-ring) and C–O (COCO-ring) σ-type bonding orbitals, respectively. As a result, the C–N and C–O bonding will be strengthened with the overlap contribution from the neighboring π-bonding orbitals. In fact, the C–O (1.404 Å) and C–N (1.400 Å) bond

lengths are shorter than the respective typical single bonds (*i.e.*, 1.421 Å in CH₃OH and 1.467 Å in CH₃NH₂ computed at the B3LYP/6-311G(2d,d,p) level). Reasonably, the N–N bond (1.269 Å) is slightly elongated compared to the typical double bond (1.241 Å in *trans*-HNNH), due to the electron-delocalization.
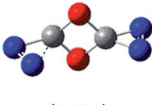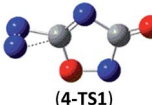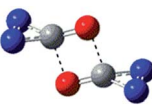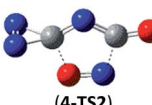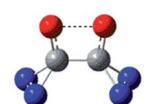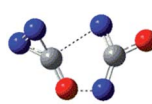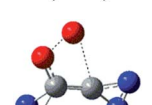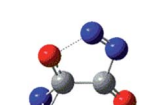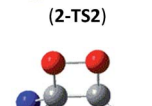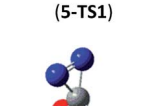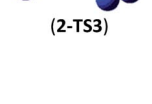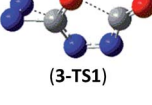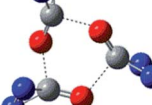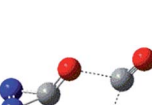
From the kinetic and electronic analysis, we can infer that the C=O/C=O *trans*-addition to form dimer **1** with all C–O single bonds while retaining the N=N bonding is a quite preferable choice. The unique spiral structure induces the effective bonding between the π orbitals (N=N or O-lone pair) and the spiral σ orbitals (C–O or C–N). Besides, the energetic feature of **1** is well kept since it lies just by 3.4 kcal mol^{-1} below 2cyc-N₂CO. The overall energy release from **1** to 2N₂ + 2CO is as huge as 168.7 kcal mol^{-1} at the CBS-QB3 level. In light of the kinetic stability criterion threshold (30 kcal mol^{-1}),[36] the dimeric isomer **1** fully meets the two strict requirements of HEDM and has the great hope to be an energetic molecule.

3.2 Oligomers of (*cyc*-N₂CO)$_n$ (n = 3–8)

The successful assembly from *cyc*-N₂CO monomer to the dimer **1** promptly encourages us to wonder whether higher-order oligomers in a similar mode can be feasible or not. Herein, we computed the trimer and tetramer of *cyc*-N₂CO *via* the C=O/C=O bond addition, *i.e.*, (*cyc*-N₂CO)$_n$ (n = 3, 4) with N=N bond still kept. Various decomposition channels were also considered. Similar to isomer **1**, the rate-determining step for trimer and tetramer is the N₂-leaving with the barriers of 25.8 and 30.3 kcal mol^{-1} at the CBS-QB3 level, respectively. For even higher-order *cyc*-N₂CO oligomers (n = 5, 6, 7, 8), the expensive CBS-QB3 calculations are very unlikely. Fortunately, we can find that the average deviation of the rate-determining barrier is only 1.9 kcal mol^{-1} between the B3LYP/6-311G(2d,d,p) and CBS-QB3 values for the small oligomers (n = 2–4) in Table 2. So for (*cyc*-N₂CO)$_n$ (n = 5–8), we used the B3LYP/6-311G(2d,d,p) results for evaluation of the kinetic stability of the designed structures. Their respective key N₂-leaving barriers are 27.2, 34.0, 24.3 and 27.0 kcal mol^{-1}, indicative of high feasibility as molecular HEDMs.

Table 2 The decomposition pathways and barriers (kcal mol^{-1}) for isomers **1–5**, trimer and tetramer of cyc-N$_2$CO at the B3LYP/6-311G(2d,d,p) (CBS-QB3) level

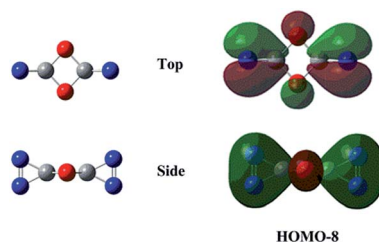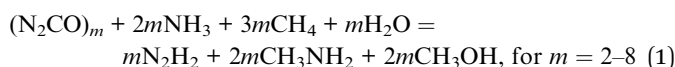| Isomers	Decomposition pathways	Structures of transition state	Barriers	Isomers	Decomposition pathways	Structures of transition state	Barriers
Isomer **1**	**1** → N$_2$ + N$_2$COCO → 2N$_2$ + 2CO	(1-TS1)	31.4 (29.9)	Isomer **4**	**4** → N$_2$ + 2NCO	(4-TS1)	2.8 (−1.7)
	1 → 2cyc-N$_2$CO	(1-TS2)	39.8 (42.9)		**4** → NO + N$_2$CNCO → NO + cyc-CNN + NCO	(4-TS2)	4.3 (8.4)
Isomer **2**	**2** → 2N$_2$ + 2CO	(2-TS1)	21.1 (19.8)		**4** → cyc-N$_2$CO + N$_2$CO	(4-TS3)	103.8 (102.9)
	2 → N$_2$C$_2$N$_2$O$_2$	(2-TS2)	59.7 (61.8)	Isomer **5**	**5** → N$_2$ + CO + cyc-N$_2$CO	(5-TS1)	0.32 (0.96)
	2 → N$_2$ + N$_2$COCO → 2N$_2$ + 2CO	(2-TS3)	23.1 (22.0)	trimer	trimer → N$_2$ + N$_4$C$_3$O$_3$	(trimer-TS1)	26.4 (25.8)
Isomer **3**	**3** → N$_2$ + 2NCO	(3-TS1)	17.9 (22.2)		trimer → 3cyc-N$_2$CO	(trimer-TS2)	57.1 (66.4)
	3 → N$_2$CO + N$_2$ + CO	(3-TS2)	35.6 (36.3)	tetramer	tetramer → N$_2$ + N$_6$C$_4$O$_4$	(tetramer-TS1)	30.6 (30.3)
	3 → CO$_2$ + N$_4$O → CO$_2$ + N$_2$ + cyc-CNN	(3-TS3)	42.7 (46.7)		tetramer → 4cyc-N$_2$CO	(tetramer-TS2)	71.6 (86.0)
	3 → CO$_2$ + N$_2$ + cyc-CNN	(3-TS4)	41.1 (44.4)				

Fig. 1 Representative valence molecular orbitals of isomer **1** at the B3LYP/6-311G(2d,d,p) level.

3.3 The detonation properties and impact sensitivity for $(cyc\text{-}N_2CO)_n$ $(n = 2–8)$

It is well known that ideal energetic materials not only require high thermal and kinetic stabilities but also exhibit an excellent detonation properties (density $\rho \approx 1.9$ g cm^{-3}, detonation velocity $D \approx 9.0$ km s^{-1}, $P \approx 40.0$ GPa), and insensitivities ($h_{50} > 12$ cm).[37] To provide detailed information for future experimental study, we computed various detonation properties of $(cyc\text{-}N_2CO)_n$ $(n = 2–8)$. For comparison, the properties of the known species like $(N_3)_2CO$, 1,3,5-trinitro-1,3,5-triazinane (RDX) and 1,3,5,7-tetranitro-1,3,5,7-tetrazocane (HMX) were also provided.

The enthalpy of formation of $(cyc\text{-}N_2CO)_n$ $(n = 2–8)$ in the gas phase (HOF$_\text{gas}$) was determined using the isodesmic reactions of reaction (1) and the known enthalpies of formation of NH$_3$(g), CH$_4$(g), H$_2$O(g), cis-N$_2$H$_2$(g), CH$_3$NH$_2$(g), and CH$_3$OH(g) taken from the NIST Chemistry Webbook.[38]

$$(N_2CO)_m + 2m NH_3 + 3m CH_4 + m H_2O =$$
$$m N_2H_2 + 2m CH_3NH_2 + 2m CH_3OH, \text{ for } m = 2–8 \quad (1)$$

Surely, to estimate the detonation performance of the title compounds, it's desirable to calculate the solid phase heats of formation (HOF$_\text{solid}$). According to Hess's law,[39] HOF$_\text{solid}$ can be obtained by

$$HOF_\text{solid} = HOF_\text{gas} - HOF_\text{sub} \quad (2)$$

where the predicted heat of sublimation (HOF$_\text{sub}$) can be represented by Rice $et\ al.$[40]

$$HOF_\text{sub} = \alpha A^2 + \beta(v\sigma_\text{total}^2)^{1/2} + \gamma \quad (3)$$

A means the surface area of the isosurface of the 0.001 electrons per Bohr^3 electronic density; v shows the degree of balance between the positive and negative potentials on the isosurface; σ_total^2 is a measure of variability of the electrostatic potential; the coefficients α, β, and γ are determined to be $\alpha = 2.670 \times 10^{-4}$ kcal mol^{-1} A^{-4}, $\beta = 1.650$ kcal mol^{-1}, and $\gamma = 2.966$ kcal mol^{-1}. The computational procedures proposed by Bulat $et\ al.$[41] were used to compute the descriptors A, v, and σ_total^2. The related data in the equation ($e.g.$ A, v, and σ_total^2.) are calculated by Lu's procedure.[42] For details, see Table S9 in ESI.†

Table 3 lists the ΔE_0, ΔE_ZPE, ΔH_T, HOF$_\text{gas}$, HOF$_\text{sub}$ and HOF$_\text{solid}$ of the title compounds at the B3LYP/6-311G(2d,d,p)

and CBS-QB3 (when available) levels. The HOF$_\text{solid}$ values of $(cyc\text{-}N_2CO)_n$ $(n = 2–8)$ are quite large and positive (387.58–1291.05 kJ mol^{-1}) (see Table 3), which are much larger than the experimentally determined values for the classic energetic materials ($i.e.$, RDX = 79.1 ± 5 kJ mol^{-1}, HMX = 75 kJ mol^{-1}).[38]

The detonation velocity (D in km s^{-1}) and detonation pressure (P in GPa) of the title compounds are estimated by the eqn (4) and (5)[43]

$$D = 1.01(N\bar{M}^{0.5}Q^{0.5})^{0.5}(1 + 1.3\rho) \quad (4)$$

$$P = 1.558\rho^2 N\bar{M}^{0.5}Q^{0.5} \quad (5)$$

N is the number of moles of gas produced per gram of explosive, and $\bar{M}$ is the mean molecular weight of the gaseous detonation products. Q is the heats of detonation (cal g^{-1}). ρ is the density of the explosive (g cm^{-3}). To obtain the theoretical density, we applied an improved equation proposed by Politzer $et\ al.$[44] in which the interaction index $v\sigma_\text{tot}^2$ is:

$$\rho = \alpha\left(\frac{M}{V(0.001)}\right) + \beta v(\sigma_\text{tot}^2) + \gamma \quad (6)$$

M is the molecular mass (g mol^{-1}) and $V(0.001)$ is the volume of the 0.001 electrons bohr^3 contour of electronic density of the molecule (cm^3 per molecule). The coefficients α, β, and γ are 0.9183, 0.0028, and 0.0443, respectively. In addition, Table 4 presents the computed detonation properties of classic energetic materials RDX and HMX, which agree consistently with experimental data.[2]

For the characteristic height (h_{50}), it is usually computed by dropping a given mass upon a sample of the compound and determining the height from which 50% of the drops produce evidence of reaction. The greater the value of h_{50}, the less is the sensitivity. h_{50} of a compound is estimated by the eqn (7).[45]

$$h_{50} = \alpha\sigma_+^2 + \beta v + \gamma \quad (7)$$

In eqn (7), the coefficient α, β, and γ, were estimated by Pospíšil $et\ al.$ as $\alpha = -0.0064$, $\beta = 241.42$, and $\gamma = -3.43$.[45] σ_+^2 is the indicator of the strengths and variabilities of the positive surface potentials, v is the degree of balance between positive and negative potential on the molecular surface.

The h_{50} values of $(cyc\text{-}N_2CO)_n$ $(n = 2–8)$ are between 33 cm and 42 cm, which are somewhat higher than those of RDX (26 cm) and HMX (29 cm)[46] (see Table 4). According to ref. 5 and 6, $(N_3)_2CO$ has the huge energy release (-116.6 kcal mol^{-1} to N$_2$ + CO), the very high decomposition barrier ($ca.$ 30 kcal mol^{-1}) and the big HOF value ($ca.$ 460 kcal mol^{-1}), making it an ideal nitrogen-rich HEDM. In our work, we found that the monomer $cyc\text{-}N_2CO$ is inferior to $(N_3)_2CO$ in view of its density ($\rho = 1.58$ g cm^{-3}), detonation velocity ($D = 7.64$ km s^{-1}) and detonation pressure ($P = 23.86$ GPa). It is ascribed to the less nitrogen-content in $cyc\text{-}N_2CO$ than in $(N_3)_2CO$. Thus, quite promisingly, with the increased oligomeric degree, the molecules $(cyc\text{-}N_2CO)_n$ have much better ρ, D, P and HOF values while retaining the appreciable kinetic stability. This indicates the effectiveness of such a simple bottom-up strategy.

Table 3 Calculated total energies (E_0), zero-point energies (E_{ZPE}), thermal corrections (H_T), and heats of formations (HOFs) of the reference compounds at the B3LYP/6-311G(2d,d,p) (CBS-QB3) level. The experimental data in square brackets [] are derived from ref. 38

Compound	E_0 (a.u.)	E_{ZPE} (a.u.)	H_T (a.u.)	HOF$_{gas}$ (kJ mol^{-1})	HOF$_{sub}$ (kJ mol^{-1})	HOF$_{solid}$ (kJ mol^{-1})
N_2	−109.55593016 (−109.398445)					
CO	−113.34623537 (−113.182005)					
NH_3	−56.57603536 (−56.460190)	0.034295	0.003809	[−45.90]		
CH_4	−40.53374825 (−40.409988)	0.044604	0.003812	[−74.90]		
H_2O	−76.44744792 (−76.337482)	0.021325	0.003779	[−241.83]		
cis-N_2H_2	−110.6634661 (−110.476252)	0.027484	0.003805	[212.97]		
CH_3NH_2	−95.88843875 (−95.668474)	0.063803	0.004354	[−23.50]		
CH_3OH	−115.7573935 (−115.539952)	0.051106	0.004259	[−215.00]		
cyc-N_2CO	−222.77096796 (−222.433774)	0.014878	0.004238	222.44 (229.09)	58.25	164.19 (170.84)
(cyc-$N_2CO)_2$	−445.5473301 (−444.891981)	0.035233	0.00659	437.67 (408.96)	50.09	387.58 (358.87)
(cyc-$N_2CO)_3$	−668.3643105 (−667.384038)	0.054587	0.009638	545.45 (490.63)	63.01	482.44 (427.61)
(cyc-$N_2CO)_4$	−891.152937 (−889.849912)	0.073222	0.012833	726.18 (641.42)	75.21	650.97 (566.22)
(cyc-$N_2CO)_5$	−1113.938994	0.091676	0.016232	913.71	90.95	822.76
(cyc-$N_2CO)_6$	−1336.722905	0.11003	0.019736	1092.02	109.65	982.37
(cyc-$N_2CO)_7$	−1559.510599	0.128457	0.023221	1287.80	129.41	1158.39
(cyc-$N_2CO)_8$	−1782.30456	0.146957	0.026912	1455.47	164.42	1291.05
RDX	−897.6546332	0.142515	0.155164	212.72 (188.98) [192]	94.19 [134.3]	118.53 (94.79) [79.5 ± 5]
HMX	−1196.874372	0.190869	0.208291	282.48 [no available]	119.17 [no available]	163.31 [75]

3.4 Implications

Overall, starting from a kinetically stable HEDM seed, *i.e.*, cyc-N_2CO, we can design novel and more complicated HEDMs (cyc-$N_2CO)_n$ (n = 2–8) that contain a cross-linked (CO)$_n$ ring and n spiral CNN rings. It is worth noting that the strategy of substituting the frameworks or ligands of known HEDMs has been frequently used and shown very effectively in generation of new and more complex HEDMs. The present strategy widens the possibility of predicting new forms of HEDMs.

In addition, within the presently designed HEDMs, the C=O bonds within cyc-N_2CO are fully transformed into the C–O single bonds, whereas the exocyclic N=N bonds are almost untouched. These species differ much from previously reported polymeric ($N_2CO)_n$ that are expected to be viable at high pressure and contain all single bonds.[29] Surely, in view of the energy storage, the ($N_2CO)_n$ with all single bonds are superior to our (cyc-$N_2CO)_n$ with partial single bonds. Yet in view of the kinetic stability, our (cyc-$N_2CO)_n$ should be quite attractive. In our model calculations of (cyc-$N_2CO)_2$, we found that activation of the N=N bond would very easily induce the N_2-extrusion. So, if the N=N activation is caused one by one during the polymerization of cyc-N_2CO, we believe that the polymeric forms with all single bonds could not be formed. Of course, this does not exclude the formation of polymeric cyc-N_2CO in a very short time scale under extreme conditions. Our work presents the first chemically feasible ($N_2CO)_n$ of HEDM interest.

We believe that our bottom-up assembly strategy would be general to apply to the other units with multiple bonds. For example, there have been growing molecular HEDMs that have been experimentally characterized, *e.g.*, $(N_3)_2C=O$,[47] $(N_3)_3P=O$,[48] and $(N_3)_2SO_2$.[49] Their suitably oligomerized compounds should provide new HEDM candidates. We are now studying the stability and detonation properties of their oligomers.

Table 4 Calculated detonation properties, release of heats, and h_{50} of title compounds, RDX, and HMX at the B3LYP/6-311G(2d,d,p) (CBS-QB3) level. The experimental data are given in square brackets []

Species	ρ (g cm^{-3})	D (km s^{-1})	P (GPa)	Release of heats (decomposition products of N_2 + CO) (kcal mol^{-1})	h_{50} (cm)
cyc-N_2CO	1.58	7.64 (7.67)	23.86 (24.08)	−82.3	50.90
(cyc-$N_2CO)_2$	1.66	8.04 (7.97)	27.30 (26.79)	−161.3	38.29
(cyc-$N_2CO)_3$	1.75	8.15 (8.05)	28.96 (28.21)	−214.7	41.55
(cyc-$N_2CO)_4$	1.76	8.19 (8.07)	29.34 (28.47)	−286.0	38.78
(cyc-$N_2CO)_5$	1.76	8.22	29.55	−358.8	34.30
(cyc-$N_2CO)_6$	1.78	8.27	30.09	−433.0	35.02
(cyc-$N_2CO)_7$	1.78	8.28	30.20	−504.9	33.05
(cyc-$N_2CO)_8$	1.79	8.28	30.30	−572.8	35.04
$(N_3)_2CO$	[1.71]^a			−116.6	54.62
RDX	1.77 [1.82]^b	8.81 (8.76) [8.75]^b	34.13 (33.73) [34.00]^b		43 [26]^c
HMX	1.80 [1.91]^b	8.91 (9.10)^b	35.23 (39.00)^b		31 [29]^c

^{a} Ref. 6. ^{b} Ref. 2. ^{c} Ref. 46.

4. Conclusion

We have presented the first theoretical design on a set of (*cyc*-$N_2CO)_n$ ($n = 2–8$) as molecular HEDMs *via* a bottom-up strategy. The kinetically most stable isomer of each oligomer is formed *via* the direct C=O/C=O *trans*-addition. In these isomers, all the C=O bonds are transformed into C–O single bonds, whereas the N=N bonds are unchanged. The unique spiral structure contributes to their good kinetic stability that are around 25–30 kcal mol^{-1}. Besides, the designed (*cyc*-$N_2CO)_n$ ($n = 2–8$) possess excellent detonation properties and low impact sensitivity. Therefore, they deserve to be viewed as very promising molecular HEDMs. Our designed candidates are structurally different from the high-pressure polymerized $(N_2CO)_n$ since the latter have all multiple bonds transformed into single bonds. The new HEDM molecules warmly welcome future laboratory studies.

Acknowledgements

References

1 T. M. Klapötke, *High Energy Density Materials, Structure and Bonding, no. 125*, New York, 2007.

2 M. B. Talawar, R. Sivabalan, T. Mukundan, H. Muthurajan, A. K. Sikder, B. R. Gandhe and A. Subhananda Rao, *J. Hazard. Mater.*, 2009, **161**, 589.

3 G. Bélanger-Chabot, M. Rahm, R. Haiges and K. O. Christe, *Angew. Chem., Int. Ed.*, 2015, **54**, 11730.

4 S. Naserifar, S. Zybin, C. C. Ye and W. A. Goddard III, *J. Mater. Chem. A*, 2016, **4**, 1264.

5 D. W. Ball, *Comput. Theor. Chem.*, 2011, **965**, 176.

6 T. Yu and B. Wu, *Inorg. Chem. Front.*, 2015, **2**, 991.

7 X. Y. Liu, Z. Y. Su, W. X. Ji, S. P. Chen, Q. Wei, G. Xie, X. W. Yang and S. L. Gao, *J. Phys. Chem. C*, 2014, **118**, 23487.

8 M. Tian, W. J. Chi, Q. S. Li and Z. S. Li, *RSC Adv.*, 2016, **6**, 47607.

9 J. H. Zhang and J. M. Shreeve, *J. Am. Chem. Soc.*, 2014, **136**, 4437.

10 K. Hafner, T. M. Klapötke, P. C. Schmid and J. Stierstorfer, *Eur. J. Inorg. Chem.*, 2015, **17**, 2794.

11 F. G. Li, Y. G. Bi, W. Y. Zhao, T. L. Zhang, Z. N. Zhou and L. Yang, *Inorg. Chem.*, 2015, **54**, 2050.

12 L. H. Tang, S. Y. Bao, J. H. Peng, K. Li, P. Ning, H. B. Guo, T. T. Zhu, J. J. Gua and Q. S. Li, *Chem. Phys. Lett.*, 2015, **639**, 166.

13 P. He, J. G. Zhang, K. Wang, X. Yin, X. Jin and T. L. Zhang, *Phys. Chem. Chem. Phys.*, 2015, **17**, 5840.

14 P. Yin, Q. H. Zhang and J. M. Shreeve, *Acc. Chem. Res.*, 2016, **49**, 4.

15 S. Zhang, Y. Qi, X. Y. Liu, X. N. Qu, Q. Wei, G. Xie, S. P. Chen and S. L. Gao, *Coord. Chem. Rev.*, 2016, **307**, 292.

16 L. Y. Yan, S. H. Gou, Z. B. Ye, S. H. Zhang and L. H. Ma, *Chem. Commun.*, 2014, **50**, 12847.

17 L. G. Bettini, F. D. Foglia, P. Milani and P. Piseri, *Int. J. Hydrogen Energy*, 2015, **40**, 6013.

18 J. Chen, H. L. Zhou and X. Feng, *Inorg. Chem.*, 2016, **55**, 4695.

19 A. A. Korkin, P. v. R. Schleyer and R. J. Boyd, *Chem. Phys. Lett.*, 1994, **227**, 312.

20 A. A. Korkin, J. Leszczynski and R. J. Bartlett, *J. Phys. Chem.*, 1996, **100**, 19840.

21 G. de Petris, F. Cacace, R. Cipollini, A. Cartoni, M. Rosi and A. Troiani, *Angew. Chem., Int. Ed.*, 2005, **44**, 462.

22 R. A. Moss, G. S. Chu and R. R. Sauers, *J. Am. Chem. Soc.*, 2005, **127**, 2408.

23 R. A. Moss and R. R. Sauers, *Tetrahedron Lett.*, 2010, **51**, 3266.

24 C. J. Shaffer, B. J. Esselman, R. J. McMahon, J. F. Stanton and R. C. Woods, *J. Org. Chem.*, 2010, **75**, 1815.

25 A. Perrin, X. Q. Zeng, H. Beckers and H. Willner, *J. Mol. Spectrosc.*, 2011, **269**, 30.

26 X. Q. Zeng, H. Beckers, H. Willner and J. F. Stanton, *Angew. Chem., Int. Ed.*, 2011, **50**, 1720.

27 X. Q. Zeng, H. Beckers, H. Willner and J. F. Stanton, *Eur. J. Inorg. Chem.*, 2012, **21**, 3403.

28 Z. Raza, C. J. Pickard, C. Pinilla and A. M. Saitta, *Phys. Rev. Lett.*, 2013, **111**, 235501.

29 C. Y. Zhu, Q. Li, Y. Y. Zhou, M. Zhang, S. T. Zhang and Q. Li, *J. Phys. Chem. C*, 2014, **118**, 27252.

30 H. M. Li, D. Q. Li, X. Q. Zeng, K. Liu, H. Beckers, H. F. Schaefer III, B. J. Esselman and R. J. McMahon, *J. Phys. Chem. A*, 2015, **119**, 8903.

31 B. B. Xie, L. H. Liu, G. L. Cui, W. H. Fang, J. Cao, W. Feng and X. Q. Li, *J. Chem. Phys.*, 2015, **143**, 194107.

32 (*a*) M. J. Frisch, G. W. Trucks, H. B. Schlegel, G. E. Scuseria, M. A. Robb, J. R. Cheeseman, J. A. Montgomery Jr T. Vreven, K. N. Kudin, J. C. Burant, J. M. Millam, S. S. Iyengar, J. Tomasi, V. Barone, B. Mennucci, M. Cossi, G. Scalmani, N. Rega, G. A. Petersson, H. Nakatsuji, M. Hada, M. Ehara, K. Toyota, R. Fukuda, J. Hasegawa, M. Ishida, T. Nakajima, Y. Honda, O. Kita, H. Nakai, M. Klene, X. Li, J. E. Knox, H. P. Hratchian, J. B. Cro, V. Bakken, C. Adamo, J. Jaramillo, R. Gomperts, R. E. Stratmann, O. Yazyev, A. J. Austin, R. Cammi, C. Pomelli, J. W. Ochterski, P. Y. Ayala, K. Morokuma, G. A. Voth, P. Salvador, J. J. Dannenbe, V. G. Zakrzewski, S. Dapprich, A. D. Daniels, M. C. Strain, O. Farkas, D. K. Malick, A. D. Rabuck, K. Raghavachari, J. B. Foresman, J. V. Ortiz, Q. Cui, A. G. Baboul, S. Clifford, J. Cioslowski, B. B. Stefanov, G. Liu, A. Liashenko, P. Piskorz, I. Komaromi, R. L. Martin, D. J. Fox, T. Keith, M. A. Al-Laham, C. Y. Peng, A. Nanayakkara, M. Challacombe, P. M. W. Gill, B. Johnson, W. Chen, M. W. Wong, C. Gonzalez and J. A. Pople, *Gaussian 09, Revision D.01*, Gaussian, Inc., Wallingford, CT, 2004; (*b*) M. J. Frisch, G. W. Trucks, H. B. Schlegel, G. E. Scuseria, M. A. Robb, J. R. Cheeseman, G. Scalmani, V. Barone, B. Mennucci, G. A. Petersson, H. Nakatsuji, M. Caricato, X. Li, H. P. Hratchian, A. F. Izmaylov, J. Bloino, G. Zheng, J. L. Sonnenberg, M. Hada, M. Ehara, K. Toyota,

R. Fukuda, J. Hasegawa, M. Ishida, T. Nakajima, Y. Honda, O. Kitao, H. Nakai, T. Vreven, J. A. Montgomery Jr, J. E. Peralta, F. Ogliaro, M. Bearpark, J. J. Heyd, E. Brothers, K. N. Kudin, V. N. Staroverov, R. Kobayashi, J. Normand, K. Raghavachari, A. Rendell, J. C. Burant, S. S. Iyengar, J. Tomasi, M. Cossi, N. Rega, J. M. Millam, M. Klene, J. E. Knox, J. B. Cross, V. Bakken, C. Adamo, J. Jaramillo, R. Gomperts, R. E. Stratmann, O. Yazyev, A. J. Austin, R. Cammi, C. Pomelli, J. W. Ochterski, R. L. Martin, K. Morokuma, V. G. Zakrzewski, G. A. Voth, P. Salvador, J. J. Dannenberg, S. Dapprich, A. D. Daniels, O. Farkas, J. B. Foresman, J. V. Ortiz, J. Cioslowski and D. J. Fox, *Gaussian 03, Revision D.02*, Gaussian, Inc., Wallingford, CT, 2009.

33 J. A. Montgomery Jr, M. J. Frisch, J. W. Ochterski and G. A. Petersson, *J. Chem. Phys.*, 1999, **110**, 2822.

34 J. A. Montgomery Jr, M. J. Frisch, J. W. Ochterski and G. A. Petersson, *J. Chem. Phys.*, 2000, **112**, 6532.

35 L. Noodleman, *J. Chem. Phys.*, 1981, **74**, 5737.

36 M. Rahm and T. Brinck, *Chem.–Eur. J.*, 2010, **16**, 6590.

37 H. M. Xiao, X. J. Xu and L. Qiu, *Theoretical Design of High Energy and Density Materials*, Science Press, Beijing, 2008.

38 http://webbook.nist.gov/chemistry/form-ser.html.

39 P. W. Atkins, *Physical chemistry*, Oxford University Press, Oxford, 1982.

40 E. F. Byrd and B. M. Rice, *J. Phys. Chem. A*, 2006, **110**, 1005.

41 F. A. Bulat, A. Toro-Labbé, T. Brinck, J. S. Murray and P. Politzer, *J. Mol. Model.*, 2010, **16**, 1679.

42 T. Lu and F. W. Chen, *J. Comput. Chem.*, 2012, **33**, 580.

43 M. J. Kamlet and S. Jacobs, *J. Chem. Phys.*, 1968, **48**, 23.

44 P. Politzer, J. Martinez, J. S. Murray, M. C. Concha and A. Toro- Labbé, *Mol. Phys.*, 2009, **107**, 2095.

45 M. Pospíšil, P. Vávra, M. C. Concha, J. S. Murray and P. Politzer, *J. Mol. Model.*, 2010, **16**, 895.

46 P. Politzer and J. S. Murray, *J. Mol. Model.*, 2015, **21**, 262.

47 X. Q. Zeng, M. Gerken, H. Beckers and H. Willner, *Inorg. Chem.*, 2010, **49**, 9694.

48 X. Q. Zeng, E. Bernhardt, H. Beckers and H. Willner, *Inorg. Chem.*, 2011, **50**, 11235.

49 X. Q. Zeng, H. Beckers, E. Bernhardt and H. Willner, *Inorg. Chem.*, 2011, **50**, 8679.